Journal for ImmunoTherapy of Cancer

CSF proteomics identifies ADGRG1 as a predictive biomarker of intrathecal immune checkpoint inhibitor response in leptomeningeal metastasis

Lishi Wang ,[1] Guozi Yang,[2] Hang Lei,[1] Yuancheng Zhang,[1] Bin Li,[3] Miaomiao Liu,[1] Yushan Huang,[1] Xiao Chen,[1] Panpan Tai,[1] Zhenyu Pan [4]

To cite: Wang L, Yang G, Lei H, *et al*. CSF proteomics identifies ADGRG1 as a predictive biomarker of intrathecal immune checkpoint inhibitor response in leptomeningeal metastasis. *Journal for ImmunoTherapy of Cancer* 2026;**14**:e013588. doi:10.1136/jitc-2025-013588

► Additional supplemental material is published online only. To view, please visit the journal online (https://doi.org/10.1136/jitc-2025-013588).

LW and GY contributed equally.

Accepted 24 January 2026

For numbered affiliations see end of article.

Correspondence to
Dr Zhenyu Pan;
dr-zypan@163.com

ABSTRACT

Background Leptomeningeal metastasis (LM) is a fatal complication of advanced cancer with limited therapeutic options and poor prognosis. Immune checkpoint inhibitors (ICIs) have shown promise in systemic disease, but intrathecal ICIs efficacy and immunological impact in LM remain unclear. Cerebrospinal fluid (CSF) proteomics may provide a unique window into the CNS immune microenvironment and enable response prediction.

Methods We enrolled 62 patients with LM who received intrathecal pemetrexed (InPe) with or without ICIs (InPe+programmed cell death protein-1 (PD-1), InPe+PD-1+cytotoxic T-lymphocyte associated protein 4 (CTLA-4), InPe+PD-1+vascular endothelial growth factor (VEGF)). Matched CSF (pretreatment and post-treatment) and pretreatment serum samples were collected for high-content proteomic profiling using the Olink platform. Differential expression, pathway enrichment, and machine learning-based modeling were applied to identify treatment-induced changes and predictive biomarkers.

Results Nearly half of the patients achieved clinical response. Post-treatment CSF showed enrichment of cytokine and chemokine signaling pathways, with a marked decrease in EGF. Adding PD-1 inhibitor restored immune cell function and upregulated interferon-γ. Compared with serum, CSF proteomic profiles provided superior predictive performance (area under the curve (AUC) 0.884 vs 0.780). A five-protein CSF signature (ADGRG1, CD28, CCL23, DCN, IL-15) achieved robust prediction (AUC 0.968 in InPe+PD-1 training cohort, 0.917 in InPe+PD-1+CTLA-4 validation cohort, and 1 in InPe+PD-1 subsequent validation cohort). ADGRG1 was significantly higher in non-responders at baseline (p=0.031) and decreased after treatment, and specific enrichment in dura-derived LM-associated macrophages, suggesting a macrophage-derived source and potential role in LM progression.

Conclusions This study provides the first high-content proteomic atlas of intrathecal ICI therapy in LM, identifies intrathecal ICI therapy-specific immune remodeling in LM, and establishes a CSF-based predictive model with high accuracy. ADGRG1 represents a promising biomarker of treatment responsiveness and a potential mechanistic link between macrophage biology and LM progression.

WHAT IS ALREADY KNOWN ON THIS TOPIC

⇒ Leptomeningeal metastasis is a devastating complication of cancer with very limited therapeutic options. Intrathecal immune checkpoint inhibitors (ICIs) show potential, but no validated cerebrospinal fluid (CSF)-based biomarkers exist, and proteomic profiling has not been systematically applied.

WHAT THIS STUDY ADDS

⇒ We report the largest leptomeningeal metastasis cohort analyzed with high-content CSF proteomics and the first to evaluate intrathecal ICI-based therapy using this approach. The study identifies ADGRG1 as a novel macrophage-associated biomarker and develops a CSF-derived predictive model with high accuracy.

HOW THIS STUDY MIGHT AFFECT RESEARCH, PRACTICE OR POLICY

⇒ CSF proteomics emerges as a practical platform for biomarker discovery and treatment stratification in leptomeningeal metastasis. These findings may guide precision immunotherapy trials and inform biomarker-driven clinical decision-making.

INTRODUCTION

Leptomeningeal metastasis (LM) represents a devastating complication of advanced malignancies, characterized by the dissemination of tumor cells to the leptomeninges and cerebrospinal fluid (CSF).[1] The therapeutic options recommended in clinical practice guidelines are limited and primarily include intrathecal chemotherapy, radiotherapy, molecular targeted therapy and palliative care.[2 3] Nevertheless, the prognosis remains dismal, with median overall survival across tumor types ranging from 2 to 6 months, even among patients responding to currently available treatments.[4]

Under physiological conditions, the central nervous system (CNS) is generally considered an immune-privileged site, where access

of immune cells to the CSF microenvironment is highly restricted.[5] The CSF is typically acellular and immunologically quiescent, predominantly populated by T cells. However, when LM occurs, the CSF immune landscape undergoes a profound transformation. In LM, the CSF exhibits a markedly inflammatory and pleocytic profile, driven by a substantial influx of both lymphoid and myeloid lineages, including T cells, natural killer cells, dendritic cells, monocytes, macrophages, and neutrophils.[6] Paradoxically, despite this robust immune infiltration, the CSF microenvironment becomes immunosuppressive, characterized by T-cell exhaustion and inactivation.[7] Consequently, the antitumor immune response is largely ineffective in controlling disease progression.

Recent advances in immunotherapy, particularly immune checkpoint inhibitors (ICIs), have transformed the management of several systemic malignancies.[8 9] By targeting inhibitory receptors such as programmed cell death protein-1 (PD-1)/programmed death-ligand 1 (PD-L1) and cytotoxic T-lymphocyte associated protein 4 (CTLA-4), ICIs can restore T-cell function and reinvigorate antitumor immunity. The route of administration is critical for the treatment of LM. When administered intravenously, due to the blood-CSF barrier (BCSFB), PD-1 inhibitors, as large-molecule ICI antibodies, are difficult to directly enter the CSF. Consequently, the drug present in the bloodstream primarily interacts with peripheral T cells located in lymph nodes, the spleen, and the circulation. Only after these T cells are activated and successfully cross the BCSFB into the CSF can they exert antitumor activity against LM. This process is generally inefficient and is further suppressed by the immunosuppressive tumor microenvironment of the CNS. In contrast, intrathecal administration of ICIs bypasses the BCSFB entirely. These immunotherapeutic agents are delivered directly into the CSF, where they can activate local immune cells including circulating T cells in the CSF and resident immune cells within the meninges, to mediate antitumor responses. Moreover, a portion of the intrathecally delivered drugs is cleared into the systemic circulation along with CSF outflow, thereby producing peripheral effects comparable to those achieved with intravenous ICIs administration. Compared with intravenous delivery, the intrathecal route offers a more direct means of drug delivery to the CSF compartment and may be associated with a trend toward improved clinical outcomes.[10 11]

Several studies have been conducted to explore the role of intrathecal ICIs in patients with LM.[10 12–14] However, the clinical responses to intrathecal ICIs for LM with solid tumors are highly variable. This underscores the urgent need for effective biomarkers to optimize patient selection. Furthermore, the immune microenvironment dynamics of LM differ from those of systemic disease, raising questions about how ICIs reshape the CNS immune milieu and which patients are most likely to benefit.

The CSF, in direct contact with LM lesions, provides a unique window into CNS tumor biology and immune activity. Compared with peripheral blood, CSF may more accurately reflect immunological changes within the CNS during treatment and therefore has greater potential for predicting treatment response. Previous studies have identified several CSF-based biomarkers with potential predictive value for LM. In particular, elevated levels of circulating tumor DNA (ctDNA) in CSF have been associated with tumor burden and poor prognosis,[15] while specific mutations detected in ctDNA (eg, EGFR, KRAS) may reflect treatment response to targeted therapies.[16] MicroRNAs (eg, miR-7977, miR-7975) and exosomes have also been implicated in LM progression and have shown promise in monitoring disease status.[17 18] CSF CEA, HE4, and CEACAM6 have promising applications for the diagnosis of LM in certain cancer types.[19 20] However, the predictive performance of these biomarkers for response to intrathecal immunotherapy remains largely unexplored, and none have been validated specifically for ICIs in LM.

Proteomic profiling offers a powerful approach to elucidate disease-specific immune landscapes and identify predictive biomarkers. Recent studies using the advanced Olink proteome technology have demonstrated the value of large-scale plasma proteome analyses in cancer patients receiving ICIs.[21 22] Compared with traditional biomarkers, such as PD-L1 expression status, circulating biomarkers offer a promising alternative by overcoming limitations associated with tumor tissue analysis, such as temporal and spatial heterogeneity.[23–25] This approach may be particularly valuable for LM, where obtaining tissue samples for PD-L1 detection is clinically challenging. Proteomic analysis of liquid biopsies (like CSF) could thus provide a unique and previously unexplored perspective on dynamic protein changes following intrathecal ICIs treatment.

Starting in February 2024, we initiated a series of clinical trials investigating intrathecal ICIs combined with chemotherapy for LM (ClinicalTrials.gov identifiers: NCT06462222, NCT06809530, NCT06809517, and NCT06762080). To capture the dynamic proteomic alterations induced by these therapies and to identify predictive biomarkers, we performed high-content proteomic profiling using the Olink platform on paired CSF and serum samples from 62 patients with LM treated with either intrathecal ICIs plus pemetrexed or pemetrexed alone. We systematically compared pretreatment and post-treatment proteomic changes, delineated regimen-specific immune pathway modulation, and identified key biomarkers associated with therapeutic response. Leveraging machine learning-based modeling, we constructed and validated a CSF-derived predictive score that achieved high accuracy in forecasting treatment outcomes, surpassing the performance of serum-based models. Notably, we discovered ADGRG1 as a novel response-associated protein and validated its expression in independent datasets.

Table 1 Baseline clinical characteristics of patients with leptomeningeal metastasis

(A) Patient and clinical characteristics	Overall
n	62
Age (median (IQR)	53 (48–58)
Gender (%)	
Male	21 (34)
Female	41 (66)
Primary tumor (%)	
Lung adenocarcinoma	47 (76)
Breast cancer	10 (16)
Gastric adenocarcinoma	4 (6)
Small-cell lung cancer	1 (2)
Treatment (%)	
InPe	17 (27)
InPe+PD-1	29 (47)
InPe+PD-1+CTLA4	10 (16)
InPe+PD-1+VEGF	6 (10)
Best response to treatment (%)	
Response (responder)	32 (52)
Stable disease (non-responder)	22 (36)
Progression (non-responder)	1 (2)
Not evaluable	6 (10)

(B) Patient and clinical characteristics				
n	Non-responder	Responder	P value	test
Age (median (IQR)	53 (48–59)	53 (48–58)	0.9933	Wilcox
Gender (%)			1	χ^2
Male	8 (35)	12 (36)		
Female	15 (65)	21 (64)		
Primary tumor			0.901	Fisher's exact
Lung adenocarcinoma	19 (83)	27 (82)		
Breast cancer	4 (17)	4 (12)		
Gastric adenocarcinoma	0 (0)	1 (3)		
Small-cell lung cancer	0 (0)	1 (3)		
Treatment (%)			0.554	Fisher's exact
InPe	5 (22)	6 (18)		
InPe+PD-1	10 (43)	19 (58)		
InPe+PD-1+CTLA4	6 (26)	4 (12)		
InPe+PD-1+VEGF	2 (9)	4 (12)		

CLA-4, cytotoxic T-lymphocyte associated protein 4; InPe, intrathecal pemetrexed ; PD-1, programmed cell death protein 1; VEGF, vascular endothelial growth factor.

METHODS

Patient samples and treatment assessment

Patients were prospectively recruited at the Affiliated Huizhou Hospital of Guangzhou Medical University. Eligible patients were aged 18–75 years with cytologically confirmed LM and a pathologically confirmed malignant solid tumor. The primary tumors included lung adenocarcinoma, small-cell lung cancer, breast cancer and gastric adenocarcinoma, as detailed in table 1. Exclusion criteria comprised hematologic malignancy, primary CNS malignancy, or any other condition unsuitable for this study, including serious CNS disorders, hydrocephalus or other factors suggestive of CSF obstruction, lethal or extensive systemic diseases with few treatment options,

psychiatric illness, or poor compliance. Enrolled patients were scheduled to receive one of four treatment regimens: intrathecal pemetrexed (InPe), intrathecal PD-1 inhibitor+pemetrexed (InPe+PD-1), intrathecal PD-1/vascular endothelial growth factor inhibitor+pemetrexed (InPe+PD-1+VEGF), or intrathecal PD-1/CTLA4 inhibitor+pemetrexed (InPe+PD-1+CTLA4). The sample size for each treatment group was determined based on feasibility and patient availability during the study period, without formal statistical power calculation due to the exploratory nature of this proteomic study. Treatment response was evaluated according to the Response Assessment in Neuro-Oncology criteria for LM.

Additionally, we subsequently collected a separate batch of CSF samples from InPe+PD-1-treated patients for model validation (online supplemental file).

This study was carried out as part of four prospective studies registered on ClinicalTrials.gov, NCT06462222, NCT06809530, NCT06809517, and NCT06762080. Approval was obtained from the Institutional Ethics Committee of the Affiliated Huizhou Hospital of Guangzhou Medical University and the study adhered to the principles of the Declaration of Helsinki. Written informed consents were obtained from all participants, indicating their willingness to donate their CSF and blood samples for research. Permission to access and publish patient information was also obtained from each patient.

Sample collection and processing

To ensure analytical validity, we followed the EuroFlow 2024 SOP for CSF handling. CSF samples were obtained via lumbar puncture or Ommaya reservoir before the first intrathecal administration and after the seventh intrathecal administration, respectively. Blood samples were collected on the same day as the baseline CSF draw prior to the first intrathecal administration. All samples were processed within 1 hour of collection. Hemoglobin was not directly quantified by Olink. However, the panel includes two erythrocyte lysis markers (HBA1/HBB) whose Normalized Protein eXpression (NPX) values were consistently below the lower limit of detection in all CSF samples, indicating absence of significant traumatic tap or in vitro hemolysis.[26 27] The CSF biochemistry of patients was detailed in table 2. CSF samples were centrifuged at 1,500 rpm for 5 min at 4°C. Blood samples collected in the clot activator tubes were centrifuged at 3,000 rpm for 10 min at 4°C. Subsequently, the upper layer of serum was obtained, aliquoted, and stored at −80°C until analysis.

Protein expression assay

Protein quantification was performed using the Olink proteomics platform immuno-oncology panel, enabling simultaneous measurement of 92 proteins related to immune signaling, cytokine, and chemokine pathways. The panel covers proteins involved in key biological processes including T-cell activation, immune checkpoint regulation, cytokine–cytokine receptor interaction, chemotaxis, apoptosis, and angiogenesis. Raw expression data were log2-transformed normalized according to the manufacturer's guidelines and expressed as NPX values. Only proteins detected in more than 50% of samples were retained for downstream analyses.

Validation of ADGRG1 expression in macrophages

To experimentally validate ADGRG1 expression in macrophages under different tumor and immunotherapy conditions, we established an in vitro co-culture system using THP-1-derived macrophages and A549 lung adenocarcinoma cells. Both cell lines were obtained from the Cell Bank of the Chinese Academy of Sciences. THP-1 cells were maintained in RPMI-1640 medium supplemented with 10% fetal bovine serum and

Table 2 CSF biochemistry of patients with leptomeningeal metastasis

(A) Cerebrospinal fluid biochemistry pre				
mean	**Non-responder**	**Responder**	**P value**	**Test**
ADA (U/L)	0.49	0.45	0.834	T-test
MTP (mg/dL)	50.26	103.42	0.027	T-test
LDH (U/L)	59.60	77.57	0.210	T-test
Cl (mmol/L)	121.47	119.55	0.106	T-test
Glu (mmol/L)	2.46	2.73	0.339	T-test
(B) Cerebrospinal fluid biochemistry				
mean	**Pre**	**Post**	**P value**	**Test**
ADA (U/L)	0.47	0.53	0.585	T-test paired
MTP (mg/dL)	81.68	69.46	0.447	T-test paired
LDH (U/L)	73.24	56.81	0.003	T-test paired
Cl (mmol/L)	119.96	118.98	0.112	T-test paired
Glu (mmol/L)	2.59	3.07	<0.001	T-test paired

ADA, adenosine deaminase; Cl, chloride; Glu, glucose; LDH, lactate dehydrogenase; MTP, total protein M.

1% penicillin-streptomycin. Differentiation into macrophages (THP-1–MΦ) was induced by treatment with phorbol 12-myristate 13-acetate (PMA, 100 ng/mL) for 48 hours, followed by replacement with PMA-free medium and incubation for an additional 24 hours to obtain stably differentiated macrophages.

For tumor-macrophage co-culture, A549 cells were seeded in the upper chamber of a 0.4–8 µm pore Transwell insert, while THP-1–MΦ were cultured in the lower chamber, allowing soluble factor exchange without direct contact. Cells were co-cultured for 48–72 hours to mimic the tumor microenvironment. Three experimental groups were established: (1) M0 group—THP-1-derived macrophages cultured alone. (2) M0+A549 group—THP-1–MΦ co-cultured with A549 cells. (3) M0+A549+PD-1 group—co-cultured as above, with anti-PD-1 antibody (10 µg/mL) (Toripalimab) added after successful PD-1 induction to simulate immune checkpoint blockade. Toripalimab was manufactured and provided by Shanghai Junshi Biosciences, Shanghai, China. Each group was cultured in triplicate, and cells from three wells were collected for statistical analysis.

After 24–48 hours of antibody treatment, cells were harvested for RNA extraction. Quantitative real-time PCR (qPCR) was performed to assess the expression levels of PDCD1 (primer-F: AAGGCGCAGATCAAAGAGAGCC; primer-R:CAACCACCAGGGTTTGGAACTG) and ADGRG1 (primer-F:TGAGACCGTCAGGAGAGAAACC; primer-R:AGGCTCAGGTAGTGCTT GTGCA), using GAPDH (primer-F:GGAGCGAGATCCCTCCAAAAT; primer-R:GGCTGTTGT CATACTTCTCATGG) as an internal control. Relative expression was calculated using the $2^{-\Delta\Delta Ct}$ method.

Healthy CSF protein comparison and batch correction

To characterize the proteomic landscape in LM CSF, we incorporated proteomic data from a multiple sclerosis cohort that included healthy control (HC) samples.[28] To minimize potential batch effects between LM and HC CSF proteomic datasets, batch correction was performed using the *ComBat* method implemented in the *sva* R package. The corrected expression matrix was then used for subsequent comparative and visualization analyses, including principal component analysis (PCA) and differential protein expression.

Pathway enrichment analysis

Differentially expressed proteins were subjected to functional enrichment analysis. Gene Ontology terms and Kyoto Encyclopedia of Genes and Genomes pathway enrichment were analyzed using the clusterProfiler R package. Enrichment results were considered significant at false discovery rate <0.05.

Predictive model construction

Top five importance genes were selected ranked by random forest (RF) for generalized linear models (GLM) to generate a predictive response score using glm function in R caret package. Model performance was assessed using receiver operating characteristic curves, with area under the curve (AUC) calculated via the pROC R package.

Statistical analysis

All statistical analyses were conducted using R software (V.4.4.1). Continuous variables were compared using the Wilcoxon rank-sum test, categorical variables with the χ^2 test or Fisher's exact test accordingly, and paired comparisons using the paired Wilcoxon signed-rank test. Differential expression compared among treatment was performed using the Kruskal-Wallis test. qPCR data were analyzed using an unpaired two-tailed Student's t-test.

Hierarchical clustering and PCA were applied to visualize proteomic differences.

Univariate Cox proportional hazards models were applied to evaluate associations between clinical features and therapeutic response.

RESULTS

Patient characteristics and treatment response

Between February 2024 and June 2025, a total of 62 patients with LM from solid tumors were enrolled, including 21 (34%) males and 41 (66%) females, with a median age of 53 years (range: 32–67). Patients were assigned to one of four treatment groups: InPe (n=17), InPe+PD-1 (n=29), InPe+PD-1+CTLA4 (n=10), and InPe+PD-1+VEGF (n=6) (figure 1A,B). Baseline clinical characteristics were balanced across the four treatment groups (table 1). Treatment responses were classified as responders (clinical response) or non-responders (stable disease or disease progression) (online supplemental file). The overall response rate was highest in the InPe+PD-1+VEGF group (67%), followed by InPe+PD-1 (66%), InPe (55%), InPe+PD-1+CTLA4 (40%) and with no significant difference among regimens (p=0.171) (figure 1C).

Forest plot analysis of ORs revealed no statistically significant associations between therapeutic response and patient age, sex (all p>0.05) (online supplemental figure S1B).

PCA revealed distinct protein profiles between CSF and serum samples (online supplemental figure S1A). We further compared the CSF proteomic features of patients with LM with publicly available HC CSF data. After batch correction (online supplemental figure S1C,D), inflammation-related and cytokine-related proteins such as CXCL9, CXCL10, CCL3, CD27, and CD8A were significantly upregulated in both pretreatment and post-treatment LM samples compared with HCs (online supplemental figure S1E,F).

Distinct CSF proteomic alterations before and after treatment for LM

When comparing pretreatment and post-treatment CSF proteomes across the four treatment regimen, one treatment group (InPe+PD-1+VEGF) showed no statistically

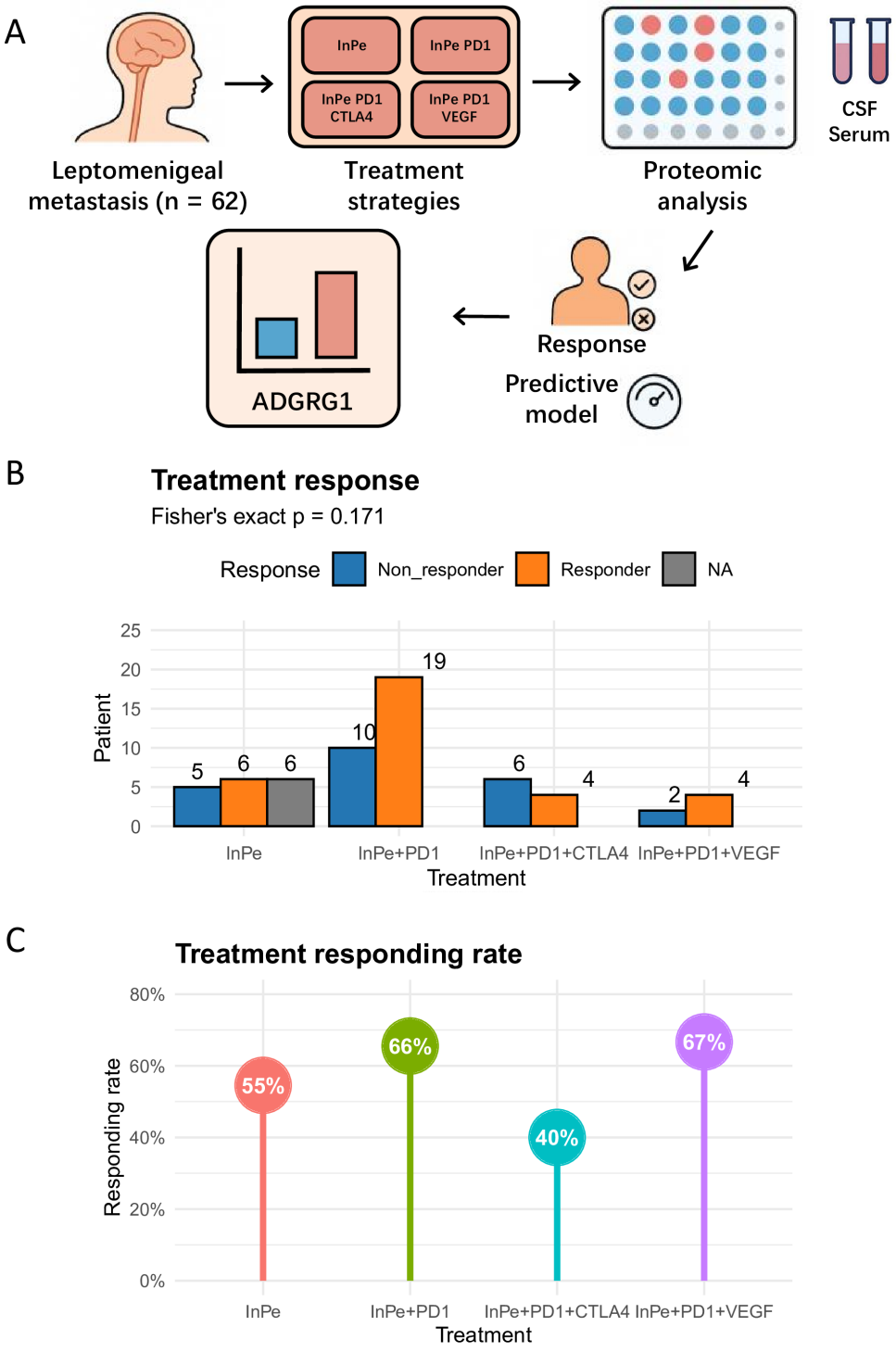

Figure 1 Patient characteristics and workflow. (A) Schematic overview of the study workflow. (B) Barplot showing clinical response categories for the four treatment regimens. (C) Lollipop plot showing clinical response rate for the four treatment groups. CTLA4, cytotoxic T-lymphocyte associated protein; InPe, intrathecal pemetrexed; PD-1, programmed cell death protein-1; VEGF, vascular endothelial growth factor.

significant differentially expressed proteins. In contrast, the other regimens exhibited both shared and regimen-specific alterations (online supplemental figure S2A–C). Common changes included a set of significantly differentially expressed proteins shared among multiple regimens (figure 2A), enrichment of cytokine and chemokine signaling pathways (figure 2G,H), and a marked reduction in EGF levels (figure 2C). Collectively, these shared alterations suggested suppression of tumor-promoting processes and restoration of antitumor immune activity.

However, regimen-specific differences were evident. MMP7 and CCL17 were downregulated only in regimens incorporating immunotherapy (InPe+PD-1 and InPe+PD-1+CTLA4) (figure 2E,F). In addition, PDCD1 was uniquely

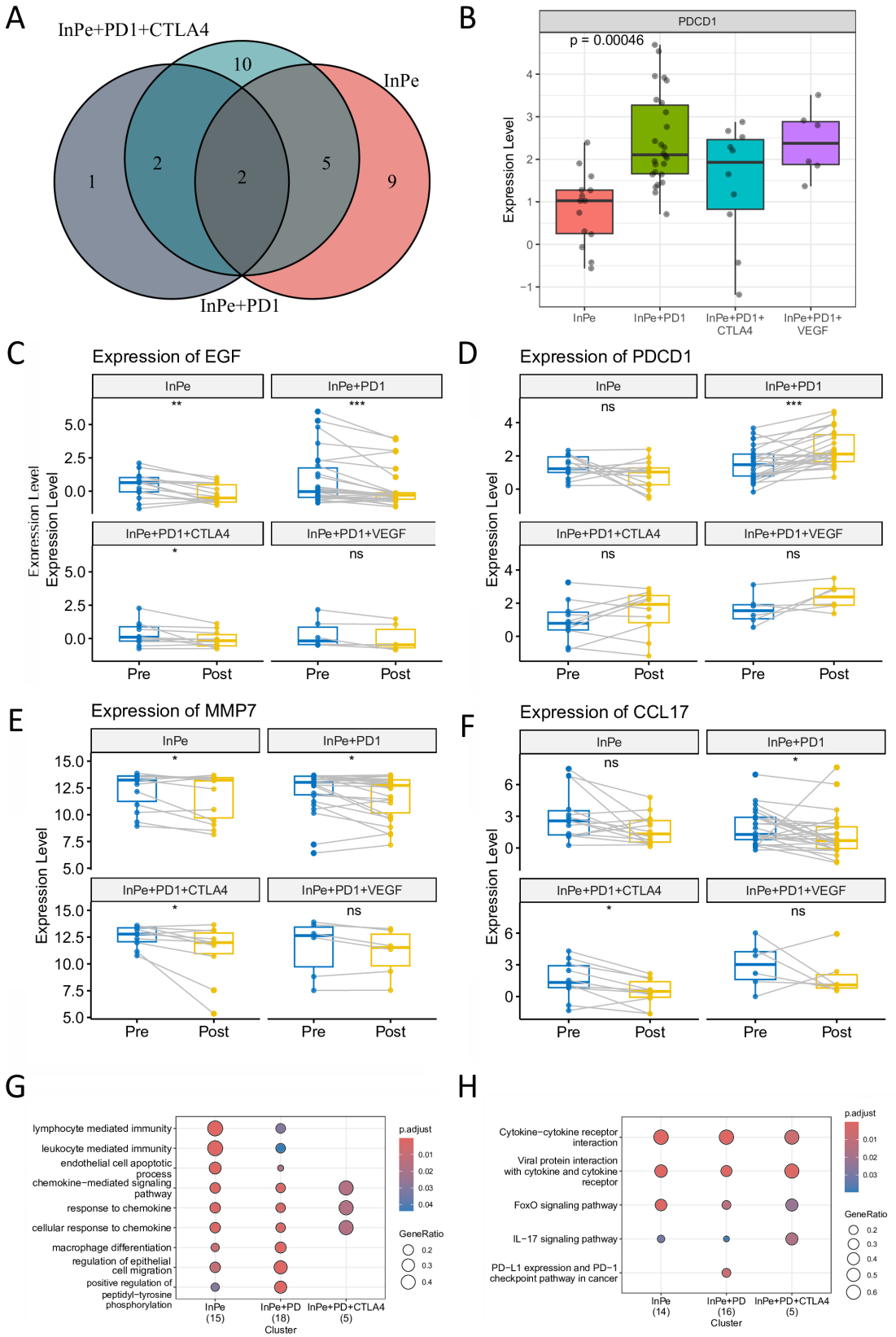

Figure 2 Proteomic alterations in CSF before and after treatment across four therapeutic regimens. (A) Venn diagram showing the overlap of differentially expressed proteins among regimens. (B) Boxplot showing PDCD1 expression levels in post-treatment CSF across regimens. (C–F) Boxplot showing pretreatment and post-treatment levels of EGF, PDCD1, MMP7, and CCL17. (G–H) Dotplot showing GO terms and KEGG enrichment. Statistical significance: ns, not significant ($p \geq 0.05$); *$p<0.05$; **$p<0.01$; ***$p<0.001$. CSF, cerebrospinal fluid; CTLA4, cytotoxic T-lymphocyte associated protein; GO, Gene Ontology; InPe, intrathecal pemetrexed; KEGG, Kyoto Encyclopedia of Genes and Genomes; PD-1, programmed cell death protein-1; VEGF, vascular endothelial growth factor.

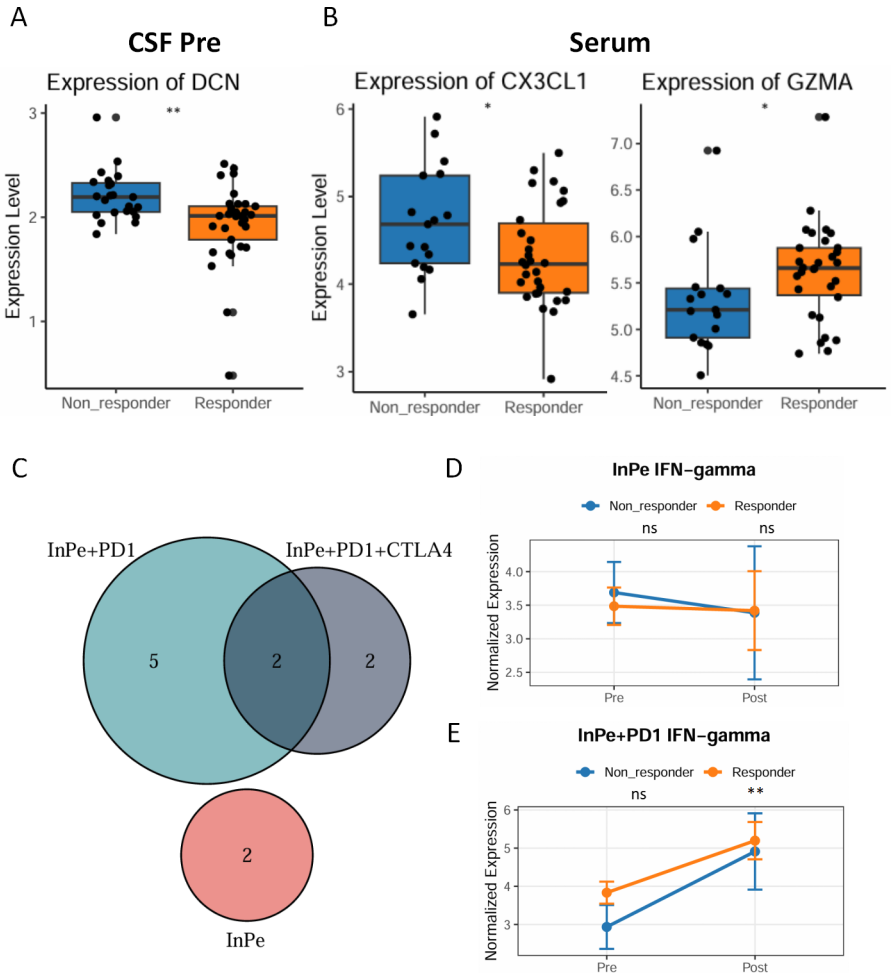

Figure 3 Protein alterations between responders and non-responders. (A) Boxplot showing DCN changes between responders and non-responders in CSF-Pre. (B) Boxplot showing CXCL1 and GZMA changes between responders and non-responders in serum. (C) Venn diagram showing the overlap of differentially expressed proteins between responders and non-responders among regimens. (D) Lineplot showing IFN-γ post-treatment alterations within responders and non-responders in InPe. (E) Line plot showing IFN-γ post-treatment alterations within responders and non-responders in InPe+PD-1. Statistical significance: ns, not significant (p≥0.05); *p<0.05; **p<0.01; ***p<0.001. CSF, cerebrospinal fluid; CTLA4, cytotoxic T-lymphocyte associated protein; DCN, decorin; IFN, interferon; InPe, intrathecal pemetrexed; PD-1, programmed cell death protein-1.

upregulated in the InPe+PD-1 group (figure 2D), and its expression level differed significantly among post-treatment CSF samples across four regimens (p=0.0025). These findings suggested that immunotherapy-containing regimens may represent distinctive immunotherapy-associated effects in LM.

Differential proteomic profiles between responders and non-responders in CSF and serum

Comparative analysis between responders and non-responders revealed distinct proteomic signatures in CSF and serum samples. Notably, the CSF proteome exhibited differential expression of DNC (figure 3A), whereas serum profiles showed distinct involvement of CXC3CL1 and GZMA (figure 3B), highlighting the compartment-specific immune landscape.

When stratified by treatment regimen, the addition of PD-1 inhibitor was associated with a significant upregulation of interferon (IFN)-γ signaling in CSF, indicative of enhanced immune activation and functional restoration (figure 3D,E). Subgroup analysis of responders demonstrated marked increases in CXCL9 levels (online supplemental figure S3A,B), and decreases in EGF levels only in the InPe+PD-1 group, a pattern absent in non-responders and in other regimens (online supplemental figure S3C,D). These findings collectively suggest that ICIs play a critical role in modulating the immune microenvironment, promoting IFN-mediated responses and improving therapeutic efficacy.

Predictive modeling of therapeutic response using proteomic features

To explore the potential of proteomic profiling for predicting treatment response, we applied a random forest algorithm to rank protein importance based on responder status. The resulting rankings differed substantially between CSF and serum datasets (online supplemental figure S4A,B). GLMs were then constructed using the top five proteins from each fluid. The CSF-based model demonstrated superior predictive performance,

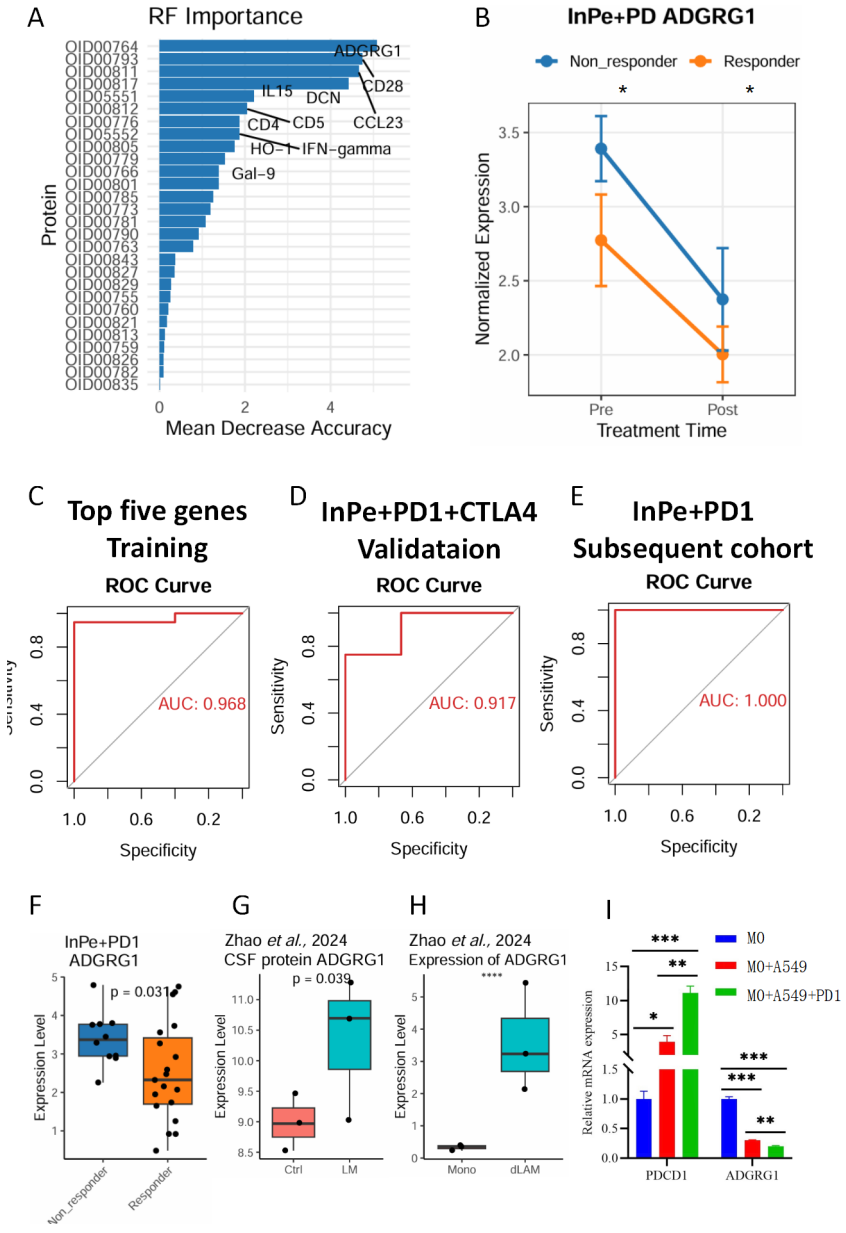

Figure 4 Construction and verification of the predictive response model in InPe+PD-1 CSF-Pre group. (A) Barplot of random forest importance. (B) Lineplot of changes in ADGRG1 expression between pretreatment and post-treatment samples in responder and non-responder from InPE+PD-1 group. (C) ROC curve of top five genes training. (D) ROC curve of InPe+PD-1+CTLA4 validation. (E) ROC curve of InPe+PD-1 subsequent validation cohort. (F) Boxplot of ADGRG1 expression comparison between responders and non-responders in InPE+PD-1 CSF-Pre samples. (G) Boxplot of CSF ADGRG1 protein levels comparison between LM and controls. (H) Boxplot of ADGRG1 gene expression comparison between dLAMs and other MΦ. (I) Barplot of PDCD1 and ADGRG1 expression in THP-1 (M0), THP-1 co-cultured with A549 cells (M0+A549), and THP-1 co-cultured with A549 cells plus anti-PD-1 (M0+A549+PD-1). Statistical significance: ns, not significant (p≥0.05); *p<0.05; ** p<0.01; ***p<0.001; ****p<0.0001. AUC, area under the curve; CSF, cerebrospinal fluid; CTLA4, cytotoxic T-lymphocyte associated protein; dLAM, dura-derived LM-associated macrophages; InPe, intrathecal pemetrexed; LM, leptomeningeal metastasis; PD-1, programmed cell death protein-1; RF, random forest; ROC, receiver operating characteristic.

achieving an AUC of 0.884, compared with 0.780 for the serum-based model (online supplemental figure S4C,D).

Given that the InPe+PD-1 group had the largest sample size, we constructed a CSF-based GLM using its top five proteins: ADGRG1, CD28, CCL23, DCN, and IL-15 (figure 4A). This model achieved an AUC of 0.968 in the training set (figure 4C). When validated in the InPe+PD-1+CTLA4 group, the model retained strong predictive accuracy with AUC of 0.917 (figure 4D). Furthermore, validation in a subsequent collected InPe+PD-1 cohort yielded an AUC of 1.000, supporting its robustness.

Among them, ADGRG1 showed a distinctive expression pattern. At baseline, its levels were significantly lower in responders compared with non-responders within the InPe+PD-1 group (p=0.031, figure 4F), and expression further declined after treatment (figure 4B).

Independent validation in the cohort reported by Zhao *et al*, 2024, confirmed that ADGRG1 was significantly upregulated in CSF from patients with LM compared with controls (p=0.039, figure 4G). Moreover, ADGRG1 expression was markedly elevated in dura-derived LM-associated macrophages (dLAMs), a macrophage population implicated in LM progression (figure 4H).

To validate the expression pattern of ADGRG1 observed in CSF proteomic profiling, we performed in vitro experiments using THP-1-derived macrophages. After co-culture with A549 tumor cells, PDCD1 expression was markedly upregulated and further increased on the addition of anti-PD-1 antibody, consistent with macrophage activation under immune checkpoint modulation (figure 4I). In contrast, ADGRG1 expression was significantly downregulated following co-culture and continued to decline after PD-1 blockade (figure 4I). These results suggest that the decreased ADGRG1 level observed in CSF after PD-1 treatment may result from reduced ADGRG1 expression in dLAMs on PD-1 inhibition.

Taken together, these results suggest that macrophages may be a source of ADGRG1, and that reduced ADGRG1 expression is associated with favorable therapeutic outcomes, highlighting its potential as an indicator of treatment responsiveness.

Correlation of response scores with immune-related proteins

To further characterize the biological context of the predictive model, we correlated its CSF-based response scores with individual protein levels. In the pretreatment CSF samples from the InPe+PD-1 cohort, 25 proteins showed significant correlations with the predicted response score (figure 5A). Stratification into high-score and low-score groups by the median revealed that several immune-activating proteins—such as IFN-γ, heme oxygenase 1 (HO-1), interleukin (IL)-6—were strongly and positively correlated with the score (figure 5B–D). Interestingly, certain immune-inhibitory proteins, including PD-L2, were also positively correlated (figure 5E), suggesting that responders may initially harbor an immunosuppressive microenvironment that is subsequently alleviated by therapy.

In the validation InPE+PD-1+CTLA4 cohort, similar correlation and stratification analyses identified distinct associations (online supplemental figure S5A–E). Notably, DCN, CX3CL1, ADGRG1, and TGF-β—all linked to tumor-promoting processes—were significantly negatively correlated with the predictive score. These results suggest that lower baseline levels of tumor-promoting mediators are associated with better predicted responsiveness in this regimen.

DISCUSSION

This study represents, to our knowledge, the largest cohort of patients with LM analyzed with high-content CSF proteomic profiling, and the first to apply such a comprehensive proteomic approach in this disease context to evaluate intrathecal ICI-based therapies. In a disease setting where therapeutic options are scarce and prognosis remains dismal, our findings highlight the value of CSF proteomics not only as a window into the LM immune microenvironment but also as a practical platform for biomarker discovery, response prediction and treatment stratification, with ADGRG1 emerging as a potential predictive indicator of therapeutic responsiveness in intrathecal ICI-based regimens.

Currently, ICIs have transformed the treatment landscape of systemic malignancies; however, their efficacy in LM remains heterogeneous, and biomarkers capable of predicting therapeutic benefit are urgently needed. While prior studies have focused on systemic biomarkers derived from serum[29–31] or tumor tissue,[32–34] there has been a lack of robust CSF-based predictors for ICI response in LM. To our knowledge, this is the first study to systematically interrogate the CSF proteome using Olink technology to identify immune-related biomarkers of response to intrathecal ICI therapy in patients with LM.

The changes in CSF proteome across different intrathecal treatment regimens may reflect the fundamental differences in the microenvironment regulation of LM under different treatment regimens. Our data reveal that post-treatment proteomic changes in CSF were both regimen-specific and partially overlapping. While the InPe+PD-1+VEGF group did not exhibit significant differential protein expression, which may be attributed to the limited sample size, the other three regimens demonstrated shared immune-related alterations, particularly involving cytokine and chemokine pathways, alongside distinct, regimen-specific changes. Given the central role of cytokines and chemokines in orchestrating antitumor immunity,[35] these findings suggest that intrathecal therapies universally engage immune responses, although through partially divergent mechanisms. Moreover, our results highlight the utility of Olink-based CSF proteomic profiling as a sensitive approach to capture these therapy-induced immune dynamics.

Of particular interest, we focused on three CSF proteins, MMP7, CCL17, and PDCD1, due to their significant association with intrathecal ICIs in LM. Previous studies demonstrate that MMP7 recruits tumor-associated neutrophils through chemokine release, thereby fostering an immunosuppressive microenvironment.[36] Similarly, CCL17 promotes immune tolerance by recruiting regulatory T cells to tumor sites and suppressing effector T-cell function.[36] The downregulation of both MMP7 and CCL17 in the CSF following intrathecal ICIs observed in this study indicates a transition from an immunosuppressive, pro-metastatic niche toward an immune-reactive microenvironment. PDCD1 (also known as PD-1) is an immune checkpoint molecule on the surface of T cells. In the early stages after intrathecal injection of ICIs, upregulation of PDCD1 in CSF was observed as a signal of immune response to treatment. PD-1 inhibitors block the binding of PD-1 to its ligands PD-L1/PD-L2, thereby reversing its inhibitory signal on T cells. Reactivated T cells highly

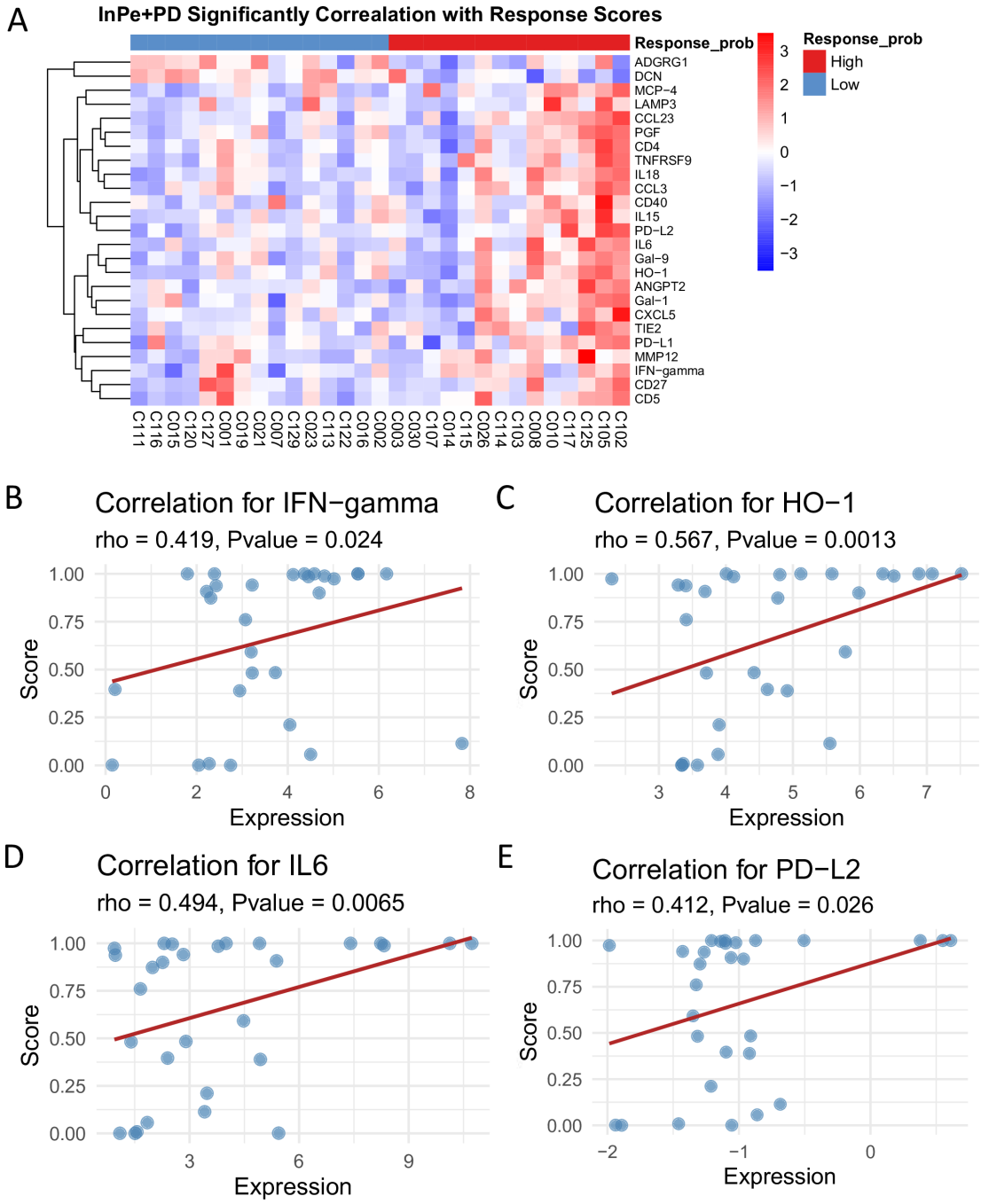

Figure 5 Correlation analysis between response scores and CSF proteins in InPe+PD-1. (A) Heatmap of significantly correlated proteins. (B–E) Correlation between response scores and IFN-gamma, HO-1, IL-6 and PD-L2. CSF, cerebrospinal fluid; IFN, interferon; HO-1, heme oxygenase 1; IL, interleukin; InPe, intrathecal pemetrexed; PD-1, programmed cell death protein-1; PD-L2, programmed death-ligand 2.

express various immune checkpoint molecules, including PD-1.[37] Moreover, PD-1 inhibitor-initiated T-cell activation enhances IFN-γ release, which subsequently upregulates PD-1 expression in the microenvironment, establishing a positive feedback loop. In our study, the addition of a PD-1 inhibitor significantly upregulated IFN-γ level in the CSF microenvironment, further corroborating this mechanistic interplay.

Comparison between responders and non-responders revealed pronounced compartment-specific differences between CSF and serum. The CSF proteome featured decorin (DCN), an extracellular matrix proteoglycan known to regulate collagen organization and modulate immune responses within the tumor microenvironment.[38–40] In contrast, the serum contained distinct markers CX3CL1, a chemokine that mediates leukocyte adhesion and trafficking,[41] and GZMA, a serine protease released by cytotoxic lymphocytes to induce target-cell apoptosis.[42] These findings suggest that CSF proteomics captures localized central nervous system immune

dynamics, whereas serum proteomics reflects more systemic immune effector activity, together providing complementary insights into treatment response.

Notably, the addition of anti-PD1 therapy led to marked upregulation of IFN-γ, a key cytokine that promotes antigen presentation, enhances cytotoxic T-cell activity, and has recently been reported to orchestrate anti-LM immune responses.[6] This was accompanied by restoration of immune cell function, consistent with the established mechanism of ICIs in reversing T-cell exhaustion. Moreover, EGF decreased and CXCL9 increased significantly only in responders receiving regimens containing a PD-1 inhibitor. Given EGF's role in driving tumor proliferation and survival,[43] and CXCL9's function as a potent T-cell chemoattractant that facilitates effector cell tracking into the tumor microenvironment,[44] these coordinated changes highlight a regiment-dependent reprogramming of the immune landscape toward a more immune-activating and tumor-suppressive state.

The predictive modeling component of our analysis demonstrated the superiority of CSF over serum in forecasting therapeutic response. Using RF-based feature ranking and generalized linear modeling, we found that CSF-based models achieved higher predictive accuracy (AUC=0.884) than serum-based models (AUC=0.780). In particular, the top five proteins identified in the therapy InPe+PD-1—ADGRG1, CD28, CCL23, DCN, and IL-15—produced excellent discrimination in both training (AUC=0.968) and validation with the InPe+PD-1+CTLA4 cohort (AUC=0.917). Functionally, these proteins represent diverse biological processes: CD28 and IL-15 mediate T-cell activation and survival,[45–48] CCL23 regulates immune cell recruitment,[49 50] DCN modulates extracellular matrix organization and immune interactions, and ADGRG1 encodes a G protein–coupled receptor. This mechanistic diversity may underlie their collective power as predictive biomarkers of therapeutic response.

To assess the reproducibility of our five-protein CSF signature across independent cohorts, we collected an additional InPe+PD-1 patient sample, which yielded a validation performance (AUC=1.000). We further compared our results with three recent proteomic studies for cross-context validation. Westrhenen *et al* conducted a QUADAS-2–compliant systematic review of 25 studies investigating CSF biomarkers for primary CNS lymphoma (PCNSL) and identified CXCL13, IL-10, sCD27, β2-microglobulin, and neopterin as the most discriminative molecules.[51] Notably, three of these—IL-10, CCL23 (same chemokine family as CXCL13), and DCN—are also components of our InPe+PD-1 predictor panel, suggesting partial convergence between ICI-responsive LM and PCNSL immune signatures. In another large-scale study, Juanes-Velasco *et al* profiled over 300 CSF samples from patients with leukemia and lymphoma with LM using liquid chromatography tandem mass spectrometry (LC-MS/MS) and affinity proteomics. Their final 19-protein LM classifier included ADGRG1, CCL23, and DCN, exactly overlapping with three of our five top hits and achieving an AUC >0.90 in their validation cohort.[52] Finally, Rossi *et al* demonstrated that minor TP53-mutated subclones (<2% Variant Allele Frequency, VAF) in the peripheral blood of patients with chronic lymphocytic leukemia predicted early chemo refractoriness and post-therapy clonal expansion.[53] As TP53 dysregulation enhances cellular migratory capacity, such subclones may represent the cellular reservoir that eventually colonizes the leptomeninges and releases ADGRG1 via dura-associated macrophages. Collectively, these external data sets validate our biomarker discovery and argue for a consensus CSF panel applicable to both lymphomatous and leukemic LM.

Among the identified markers, ADGRG1 (also known as GPR56) emerged as a particularly noteworthy candidate. ADGRG1 is an adhesion G protein-coupled receptor with emerging recognized roles in physiological processes, including brain development[54] and protecting microglial state,[55] as well as in pathological contexts, notably tumor biology.[56] Previous studies have shown that ADGRG1 can modulate cell adhesion, migration, and drug resistance.[56–58] In our cohort, ADGRG1 levels were significantly lower in responders compared with non-responders at baseline and further decreased post-treatment, suggesting that reduced expression may mark a favorable immune contexture. To further validate this finding, we conducted in vitro experiments using THP-1-derived macrophages co-cultured with A549 tumor cells to mimic the tumor microenvironment. We observed that PDCD1 expression was markedly upregulated following co-culture and further increased on anti-PD-1 antibody treatment, whereas ADGRG1 expression was significantly downregulated both after co-culture and after PD-1 blockade. Notably, as PDCD1 is also expressed on macrophages, recent evidence indicates PD-1 signaling can modulate macrophage activity and polarization.[59 60] These findings suggest that anti-PD-1 therapy may suppress ADGRG1 expression in macrophages. Importantly, as ADGRG1 protein levels in CSF also decreased after treatment, this reduction could reflect diminished ADGRG1 expression in dLAMs in response to immune checkpoint blockade. However, because CSF cellularity is markedly reduced after therapy—often nearing the limit of detection—the observed protein decline may also partly result from a decrease in total cell numbers rather than solely from transcriptional downregulation. Together, these findings suggest that macrophages, particularly dLAMs, may be a source of ADGRG1 in LM, and that reduced ADGRG1 expression could reflect diminished protumor macrophage activity after anti-PD-1 therapy, thereby creating a more favorable microenvironment for immune checkpoint blockade to act effectively.

Correlation analyses between predictive scores and protein expression provided additional mechanistic insight. In pretreatment CSF from the InPe+PD-1, both immune-activating proteins (IFN-γ, HO-1, IL-6) and PD-L2 were positively correlated with predictive scores. This may reflect an immunologically active but

checkpoint-constrained baseline state in responders, which ICIs can effectively unlock. Similarly, in the InPe+PD-1+CTLA4 cohort, tumor-promoting mediators such as DCN, CX3CL1, ADGRG1, and TGF-β were negatively correlated with predictive scores.

Despite the strengths of our study, including comprehensive CSF and serum proteomic profiling, validation across independent cohorts, and the construction of predictive models with strong discriminatory power, several limitations should be acknowledged. First, the sample size for some treatment subgroups was limited, which may reduce the generalizability of subgroup-specific findings. Given the exploratory nature of this study and the overrepresentation of lung adenocarcinoma cases, the model may exhibit a bias toward this histological subtype. Future multicenter, histology-balanced prospective studies are planned to validate the generalizability of the findings. Second, while our predictive model demonstrated robust performance in cross-validation and internal testing, we acknowledge the lack of an independent external proteomic cohort as a limitation. This is largely due to the rarity of LM and the emerging nature of intrathecal ICI therapies. To partially mitigate this, we collected an additional independent cohort of InPe+PD-1-treated patients, in which our predictive model demonstrated excellent performance (AUC=1.0). We also validated the differential expression of ADGRG1 using independent CSF proteomic datasets,[7] confirming its elevation in patients with LM compared with non-LM controls. Furthermore, cross-comparison with previously published CSF proteomic studies in lymphoma and leukemia[51–53] revealed a high degree of overlap in biomarker composition, indirectly supporting the generalizability of our five-protein CSF signature. Nevertheless, future studies with larger, multi-institutional cohorts will be essential to further confirm and refine our findings, and to establish a standardized CSF-based predictive framework for clinical application. Third, the observed post-treatment decline in CSF ADGRG1 could arise from two non-mutually exclusive mechanisms: (1) a reduction in the absolute number of dLAMs following ICI-induced immune reprogramming, or (2) downregulation of ADGRG1 expression within each remaining dLAM. Our in vitro experiments validate that macrophage ADGRG1 expression decreased after anti-PD-1 treatment. As an exploratory study, we have not yet secured the resources to perform the required single-cell or functional assays; nevertheless, such experiments are being written into our next grant and will form the basis of a subsequent mechanistic report.

CONCLUSION

In conclusion, our study provides a landmark contribution to the LM field, combining the largest cohort with the first application of high-content CSF proteomics in intrathecal ICI therapy. By integrating immune-pathway analyses, predictive modeling, and biomarker discovery, we demonstrate the potential of CSF proteomics to transform precision medicine for LM. The identification of ADGRG1 as a candidate predictive biomarker not only advances our mechanistic understanding but also opens avenues for therapeutic targeting of macrophage-driven immunosuppression.

Author affiliations
[1]Department of Radiation Oncology, The Affiliated Huizhou Hospital, Guangzhou Medical University, Huizhou, China
[2]Cancer Center, Aerospace Center Hospital, Peking University Aerospace School of Clinical Medicine, Beijing, China
[3]State Key Laboratory of Respiratory Disease Key Laboratory of Biological Targeting Diagnosis Therapy and Rehabilitation of Guangdong Higher Education Institutes, The Fifth Affiliated Hospital of Guangzhou Medical University, Guangzhou, Guangdong, China
[4]Department of Radiation Oncology, Beijing Chest Hospital, Capital Medical University, Beijing, China

Acknowledgements We thank all the group members who participate in this project.

Contributors Conceptualization, LW; methodology, LW, GY and BL; software, LW, HL and YZ; validation, LW, HL and YZ; formal analysis, LW; investigation, HL, YZ, ML, YH, XC and PT; data curation, HL, YZ, ML, YH, XC and PT; writing—original draft preparation, LW and GY; writing—review and editing, ZP; visualization, LW and GY; supervision, GY and ZP; project administration, ZP; funding acquisition, GZ and ZP; guarantor, ZP. All authors have read and agreed to the published version of the manuscript. We used ChatGPT (GPT-5, OpenAI) for text-based assistance and DALL·E (OpenAI) for schematic illustration generation. ChatGPT was used to improve clarity and grammar, ensuring concise and professional scientific writing. DALL·E was used to generate the basic shapes of schematic overviews to assemble the visually represent the study design and findings. ChatGPT assisted in refining the manuscript. Authors provided initial drafts (inputs), and ChatGPT generated revised drafts (outputs), which were then reviewed, corrected, and validated by the authors. DALL·E generated human cerebrospinal fluid, proteomic panel, tube and machine-learning model shapes based on conceptual descriptions supplied by the authors; the outputs were subsequently assembled by authors. Summary of input, output, and review: Input: Draft text, conceptual figure descriptions. Output: Refined text sections, graphical illustrations. Review: All AI-generated text and images were critically evaluated, modified as needed, and verified by the authors for accuracy, scientific validity, and appropriateness. No AI tool was used for data analysis, interpretation of results, or drawing scientific conclusions. Final responsibility for the manuscript content rests entirely with the authors.

Funding This research was funded by Huizhou Science and Technology Innovation Team Project (2023EQ050012), Guangdong Basic and Applied Basic Research Foundation, grant number (2023A1515140145), Huizhou Outstanding Young Scientific and Technological Talents Program (2025EQ050018), Guangzhou Medical University Research Ability Enhancement Project (2024SRP215). The funders had no role in study design, data collection and analysis, decision to publish, or preparation of the manuscript. The funder did not influence the results/outcomes of the study despite author affiliations with the funder.

Competing interests None declared.

Patient consent for publication Not applicable.

Ethics approval All procedures involving human participants were performed in accordance with the ethical standards of the Ethics Committee of The Affiliated Huizhou Hospital, Guangzhou Medical University (approval number: 2025-KY-019-01, 2024-KY-029-01, 2025-KY-018-01, 2025-KY-020-01). The study was conducted in accordance with the Declaration of Helsinki. Informed consent was obtained from all individual participants included in the study.

Provenance and peer review Not commissioned; externally peer reviewed.

Data availability statement Data are available in a public, open access repository. All data relevant to the study are included in the article or uploaded as supplementary information. Macrophages expression from Zhao et al,[7] Multiple sclerosis proteomics from Åkesson et al.[28]

Supplemental material This content has been supplied by the author(s). It has not been vetted by BMJ Publishing Group Limited (BMJ) and may not have been

ORCID iDs
Lishi Wang https://orcid.org/0009-0002-9416-7647
Zhenyu Pan https://orcid.org/0000-0003-0780-7758

REFERENCES

1 Wilcox JA, Chukwueke UN, Ahn M-J, *et al*. Leptomeningeal metastases from solid tumors: A Society for Neuro-Oncology and American Society of Clinical Oncology consensus review on clinical management and future directions. *Neuro Oncol* 2024;26:1781–804.
2 Naidoo J, Schreck KC, Fu W, *et al*. Pembrolizumab for patients with leptomeningeal metastasis from solid tumors: efficacy, safety, and cerebrospinal fluid biomarkers. *J Immunother Cancer* 2021;9:e002473.
3 Mack F, Baumert BG, Schäfer N, *et al*. Therapy of leptomeningeal metastasis in solid tumors. *Cancer Treat Rev* 2016;43:83–91.
4 Preusser M, Garde-Noguera J, García-Mosquera JJ, *et al*. Patritumab deruxtecan in leptomeningeal metastatic disease of solid tumors: the phase 2 TUXEDO-3 trial. *Nat Med* 2025;31:2797–805.
5 BILLINGHAM RE, BOSWELL T. Studies on the problem of corneal homografts. *Proc R Soc Lond B Biol Sci* 1953;141:392–406.
6 Remsik J, Tong X, Kunes RZ, *et al*. Interferon-γ orchestrates leptomeningeal anti-tumour response. *Nature New Biol* 2025;643:1087–96.
7 Zhao J, Zeng R, Li X, *et al*. Dura immunity configures leptomeningeal metastasis immunosuppression for cerebrospinal fluid barrier invasion. *Nat Cancer* 2024;5:1940–61.
8 Sharma P, Wagner K, Wolchok JD, *et al*. Novel cancer immunotherapy agents with survival benefit: recent successes and next steps. *Nat Rev Cancer* 2011;11:805–12.
9 Pardoll DM. The blockade of immune checkpoints in cancer immunotherapy. *Nat Rev Cancer* 2012;12:252–64.
10 Huang Y, Yang G, Liu M, *et al*. Intrathecal administration of PD-1 inhibitor combined with pemetrexed for leptomeningeal metastases from breast cancer: a case report. *Front Immunol* 2025;16:1567324.
11 Ruan Z, Zeng L, Zhang J, *et al*. Intrathecal nivolumab and IL-2 for treatment of leptomeningeal metastases in EGFR-mutated lung adenocarcinoma. *Lung Cancer (Auckl)* 2025;204:108586.
12 Glitza Oliva IC, Ferguson SD, Bassett R, *et al*. Concurrent intrathecal and intravenous nivolumab in leptomeningeal disease: phase 1 trial interim results. *Nat Med* 2023;29:898–905.
13 Zhen J, Chen L, Wang H, *et al*. Intrathecal anti-PD-1 treatment in metastatic melanoma patients with leptomeningeal disease (LMD): real-world data and evidence. *J Neurooncol* 2024;170:665–73.
14 Fan C, Hu Y, Teng C, *et al*. Intrathecal sintilimab for leptomeningeal metastases of non-small cell lung cancer failed from targeted therapy and intrathecal chemotherapy (LMIS study). *Neuro Oncol* 2025;27:1559–66.
15 Fitzpatrick A, Iravani M, Mills A, *et al*. Assessing CSF ctDNA to Improve Diagnostic Accuracy and Therapeutic Monitoring in Breast Cancer Leptomeningeal Metastasis. *Clin Cancer Res* 2022;28:1180–91.
16 Xie Y, Yang L, Fang H, *et al*. Genomic profiling and prognostic factors of leptomeningeal metastasis in EGFR-mutant NSCLC after resistant to third-generation EGFR-tyrosine kinase inhibitors. *Lung Cancer (Auckl)* 2025;205:108593.
17 Pan Z, Yang G, He H, *et al*. Identification of Cerebrospinal Fluid MicroRNAs Associated With Leptomeningeal Metastasis From Lung Adenocarcinoma. *Front Oncol* 2020;10:387.
18 Li H, Xia M, Zheng S, *et al*. Cerebrospinal fluid exosomal microRNAs as biomarkers for diagnosing or monitoring the progression of non-small cell lung cancer with leptomeningeal metastases. *Biotechnol Genet Eng Rev* 2024;40:359–80.
19 Wang Y, Luo N, Gao Y, *et al*. The joint detection of CEA and ctDNA in cerebrospinal fluid: an auxiliary tool for the diagnosis of leptomeningeal metastases in cancer. *J Cancer Res Clin Oncol* 2023;149:1679–90.
20 Li X, Chen K, Li J, *et al*. Diagnostic value of cerebrospinal fluid human epididymis protein 4 for leptomeningeal metastasis in lung adenocarcinoma. *Front Immunol* 2024;15:1339914.
21 Gao M, Wu X, Jiao X, *et al*. Prognostic and predictive value of angiogenesis-associated serum proteins for immunotherapy in esophageal cancer. *J Immunother Cancer* 2024;12:e006616.
22 Astradsson T, Sellberg F, Ehrsson YT, *et al*. Serum Proteomics in Patients with Head and Neck Cancer: Peripheral Blood Immune Response to Treatment. *Int J Mol Sci* 2022;23:6304.
23 Liu APY, Smith KS, Kumar R, *et al*. Serial assessment of measurable residual disease in medulloblastoma liquid biopsies. *Cancer Cell* 2021;39:1519–30.
24 Nikanjam M, Kato S, Kurzrock R. Liquid biopsy: current technology and clinical applications. *J Hematol Oncol* 2022;15:131.
25 Alix-Panabières C, Pantel K. Liquid Biopsy: From Discovery to Clinical Application. *Cancer Discov* 2021;11:858–73.
26 Dux R, Kindler-Röhrborn A, Annas M, *et al*. A standardized protocol for flow cytometric analysis of cells isolated from cerebrospinal fluid. *J Neurol Sci* 1994;121:74–8.
27 Chow G, Schmidley JW. Lysis of erythrocytes and leukocytes in traumatic lumbar punctures. *Arch Neurol* 1984;41:1084–5.
28 Åkesson J, Hojjati S, Hellberg S, *et al*. Proteomics reveal biomarkers for diagnosis, disease activity and long-term disability outcomes in multiple sclerosis. *Nat Commun* 2023;14:6903.
29 Ju M, Zhang J, Deng Z, *et al*. Prophylactic IL-23 blockade uncouples efficacy and toxicity in dual CTLA-4 and PD-1 immunotherapy. *J Immunother Cancer* 2024;12:e009345.
30 Zhou C, Weng J, Liu C, *et al*. Disruption of SLFN11 Deficiency-Induced CCL2 Signaling and Macrophage M2 Polarization Potentiates Anti-PD-1 Therapy Efficacy in Hepatocellular Carcinoma. *Gastroenterology* 2023;164:1261–78.
31 Gorgulho J, Loosen SH, Masood R, *et al*. Soluble and EV-bound CD27 act as antagonistic biomarkers in patients with solid tumors undergoing immunotherapy. *J Exp Clin Cancer Res* 2024;43:298.
32 Snyder A, Makarov V, Merghoub T, *et al*. Genetic basis for clinical response to CTLA-4 blockade in melanoma. *N Engl J Med* 2014;371:2189–99.
33 Sharma P, Pachynski RK, Narayan V, *et al*. Nivolumab Plus Ipilimumab for Metastatic Castration-Resistant Prostate Cancer: Preliminary Analysis of Patients in the CheckMate 650 Trial. *Cancer Cell* 2020;38:489–99.
34 Goodman AM, Kato S, Bazhenova L, *et al*. Tumor Mutational Burden as an Independent Predictor of Response to Immunotherapy in Diverse Cancers. *Mol Cancer Ther* 2017;16:2598–608.
35 Yi M, Li T, Niu M, *et al*. Targeting cytokine and chemokine signaling pathways for cancer therapy. *Signal Transduct Target Ther* 2024;9:176.
36 Maeda S, Motegi T, Iio A, *et al*. Anti-CCR4 treatment depletes regulatory T cells and leads to clinical activity in a canine model of advanced prostate cancer. *J Immunother Cancer* 2022;10:e003731.
37 Sharpe AH, Pauken KE. The diverse functions of the PD1 inhibitory pathway. *Nat Rev Immunol* 2018;18:153–67.
38 Liu J, Zhu S, Zeng L, *et al*. DCN released from ferroptotic cells ignites AGER-dependent immune responses. *Autophagy* 2022;18:2036–49.
39 Qin P, Chen H, Wang Y, *et al*. Cancer-associated fibroblasts undergoing neoadjuvant chemotherapy suppress rectal cancer revealed by single-cell and spatial transcriptomics. *Cell Rep Med* 2023;4:101231.
40 Li G, Li M, Liang X, *et al*. Identifying DCN and HSPD1 as Potential Biomarkers in Colon Cancer Using 2D-LC-MS/MS Combined with iTRAQ Technology. *J Cancer* 2017;8:479–89.
41 Herbst RS, Soria J-C, Kowanetz M, *et al*. Predictive correlates of response to the anti-PD-L1 antibody MPDL3280A in cancer patients. *Nature New Biol* 2014;515:563–7.
42 Zhong X, Zeng H, Zhou Z, *et al*. Structural mechanisms for regulation of GSDMB pore-forming activity. *Nature New Biol* 2023;616:598–605.
43 Wilson KJ, Gilmore JL, Foley J, *et al*. Functional selectivity of EGF family peptide growth factors: Implications for cancer. *Pharmacol Ther* 2009;122:1–8.
44 Meiser P, Knolle MA, Hirschberger A, *et al*. A distinct stimulatory cDC1 subpopulation amplifies $CD8^+$ T cell responses in tumors for protective anti-cancer immunity. *Cancer Cell* 2023;41:1498–515.
45 Hui E, Cheung J, Zhu J, *et al*. T cell costimulatory receptor CD28 is a primary target for PD-1–mediated inhibition. *Science* 2017;355:1428–33.

46 Yang Z, Liu X, Zhu J, *et al*. Inhibiting intracellular CD28 in cancer cells enhances antitumor immunity and overcomes anti-PD-1 resistance via targeting PD-L1. *Cancer Cell* 2025;43:86–102.
47 Patidar M, Yadav N, Dalai SK. Interleukin 15: A key cytokine for immunotherapy. *Cytokine Growth Factor Rev* 2016;31:49–59.
48 Waldmann TA, Dubois S, Miljkovic MD, *et al*. IL-15 in the Combination Immunotherapy of Cancer. *Front Immunol* 2020;11:868.
49 Gao Y, Qi F, Zhou W, *et al*. Liquid biopsy using plasma proteomics in predicting efficacy and tolerance of PD-1/PD-L1 blockades in NSCLC: a prospective exploratory study. *Mol Biomed* 2025;6:51.
50 Murata D, Azuma K, Murotani K, *et al*. Characterization of pre- and on-treatment soluble immune mediators and the tumor microenvironment in NSCLC patients receiving PD-1/L1 inhibitor monotherapy. *Cancer Immunol Immunother* 2024;73:214.
51 van Westrhenen A, Smidt LCA, Seute T, *et al*. Diagnostic markers for CNS lymphoma in blood and cerebrospinal fluid: a systematic review. *Br J Haematol* 2018;182:384–403.
52 Juanes-Velasco P, Galicia N, Pin E, *et al*. Deciphering Biomarkers for Leptomeningeal Metastasis in Malignant Hemopathies (Lymphoma/Leukemia) Patients by Comprehensive Multipronged Proteomics Characterization of Cerebrospinal Fluid. *Cancers (Basel)* 2022;14:449.
53 Rossi D, Khiabanian H, Spina V, *et al*. Clinical impact of small TP53 mutated subclones in chronic lymphocytic leukemia. *Blood* 2014;123:2139–47.
54 Giera S, Deng Y, Luo R, *et al*. The adhesion G protein-coupled receptor GPR56 is a cell-autonomous regulator of oligodendrocyte development. *Nat Commun* 2015;6:6121.
55 Zhu B, Wangzhou A, Yu D, *et al*. G-protein-coupled receptor ADGRG1 drives a protective microglial state in Alzheimer's disease through MYC activation. *Neuron* 2025;113:3224–42.
56 Ng KF, Chen TC, Stacey M, *et al*. Role of ADGRG1/GPR56 in Tumor Progression. *Cells* 2021;10:3352.
57 Luo Y, Lu J, Lei Z, *et al*. GPR56 facilitates hepatocellular carcinoma metastasis by promoting the TGF-β signaling pathway. *Cell Death Dis* 2024;15:715.
58 Zhang S, Chatterjee T, Godoy C, *et al*. GPR56 Drives Colorectal Tumor Growth and Promotes Drug Resistance through Upregulation of MDR1 Expression via a RhoA-Mediated Mechanism. *Mol Cancer Res* 2019;17:2196–207.
59 Gordon SR, Maute RL, Dulken BW, *et al*. PD-1 expression by tumour-associated macrophages inhibits phagocytosis and tumour immunity. *Nature New Biol* 2017;545:495–9.
60 Xiong H, Mittman S, Rodriguez R, *et al*. Anti-PD-L1 Treatment Results in Functional Remodeling of the Macrophage Compartment. *Cancer Res* 2019;79:1493–506.